

Supplementary Material for "Data-driven selection of the number of change-points via error rate control"

Hui Chen¹, Haojie Ren², Fang Yao^{3*} and Changliang Zou¹

¹*School of Statistics and Data Science, Nankai University, China*

²*School of Mathematical Sciences, Shanghai Jiao Tong University, China*

³*School of Mathematical Sciences, Peking University, China*

This supplementary material contains the lemmas used in the proof of Theorem 1 (Appendix C), the proofs of Proposition 1, Theorems 1–3 and Corollaries 1–2 (Appendix D–F), and some additional simulation results (Appendix G).

Appendix B: Equivalence of definitions given by Eqs.(3) and (4)

- If there exists one $k^* \in [\frac{1}{2}(j_{-1} + j); \frac{1}{2}(j + j_{+1})]$ as (3), we have $k^* - j_{-1} \geq j - k^*$ when $j \geq k^*$ or $j_{+1} - k^* > k^* - j$ when $j < k^*$, that is $|j - k^*| = \min_{l \in \mathcal{T}} |l - k^*|$ from which j follows (4);
- On the contrary, if $j = \arg \min_{l \in \mathcal{T}} |l - k^*|$ as the definition of (4), we have $k^* \geq \frac{1}{2}(j_{-1} + j)$ due to $k^* - j_{-1} > k^* - j$ if $k^* < j$; Similarly, $k^* < \frac{1}{2}(j + j_{-1})$ holds for $k^* > j$. Say, j follows the definition of (3).

*Corresponding author: fyao@math.pku.edu.cn

Appendix C: Auxiliary lemmas

Lemma S.1 *If the model (1) and Assumption 1 hold, $\hat{\Sigma}_n^{-1} = \Sigma_n^{-1} + O_p(K_n n^{-1/2})$, where Σ_n is some positive matrix depending on $\{k\}$'s.*

This lemma can be proved using the similar arguments in the Proposition 1 of Zou et al. (2020), thus the details are omitted here.

Lemma S.2 [Bernstein's inequality] *Let $X_1; \dots; X_n$ be independent centered random variables a.s. bounded by $A < \infty$ in absolute value. Let $B_n = n^{-1} \sum_{i=1}^n \mathbb{E}(X_i^2)$. Then for all $x > 0$,*

$$\Pr\left(\sum_{i=1}^n X_i \geq x\right) \leq \exp\left(-\frac{x^2}{2n B_n + 2Ax/3}\right).$$

The third one is a moderate deviation result for the mean; See Petrov (2002).

Lemma S.3 (Moderate Deviation for the Independent Sum)

Suppose that $X_1; \dots; X_n$ are independent random variables with mean zero, satisfying $\mathbb{E}(|X_j|^{2+q}) < \infty$ ($j = 1; 2; \dots$) for some $q > 0$. Let $B_n = \sum_{i=1}^n \mathbb{E}(X_i^2)$. Then

$$\frac{\Pr\left(\sum_{i=1}^n X_i > x\sqrt{B_n}\right)}{1 - \Phi(x)} \rightarrow 1 \quad \text{and} \quad \frac{\Pr\left(\sum_{i=1}^n X_i < -x\sqrt{B_n}\right)}{\Phi(-x)} \rightarrow 1;$$

as $n \rightarrow \infty$ uniformly in x in the domain $0 \leq x \leq \{\log(1/L_n)\}^{1/2}$, where $L_n = B_n^{-1-q/2} \sum_{i=1}^n \mathbb{E}(|X_i|^{2+q})$.

For notational convenience, we note that our estimation procedure can be reformulated as follows. Suppose we have two independent sets of d -dimensional observations $\{\mathbf{S}_1^O; \dots; \mathbf{S}_n^O\}$ and $\{\mathbf{S}_1^E; \dots; \mathbf{S}_n^E\}$ collected from the following multiple change-point model

$$\mathbf{S}_j^O = \boldsymbol{\mu}_k^* + \mathbf{U}_j; \quad \mathbf{S}_j^E = \boldsymbol{\mu}_k^* + \mathbf{V}_j; \quad j \in (k^*; k_{+1}^*]; \quad k = 0; \dots; K_n;$$

where $\mathbf{U}_1; \dots; \mathbf{U}_n; \mathbf{V}_1; \dots; \mathbf{V}_n$ are independent standardized noises satisfying $\mathbb{E}(\mathbf{U}_1) = \mathbf{0}$ and $\text{Cov}(\mathbf{U}_1) = \text{Cov}(\mathbf{V}_1) = \Sigma_k^*$. Let $\underline{\$} = \min_{0 \leq k \leq K_n} \text{Eig}_{\min}(\Sigma_k^*)$ and $\$ = \max_{0 \leq k \leq K_n} \text{Eig}_{\max}(\Sigma_k^*)$,

where $\text{Eig}_{\min}(\mathbf{A})$ and $\text{Eig}_{\max}(\mathbf{A})$ denote the smallest and largest eigenvalues of a square matrix \mathbf{A} . By Assumption 1, we know that $0 < \underline{\$} < \$ < \infty$. To keep the subscript consistent with the main body, we roughly let \mathbf{S}_{2j}^O , \mathbf{U}_{2i} , \mathbf{S}_{2i-1}^E , \mathbf{V}_{2i-1} as 0 for $i = 1; \dots; m$.

The next one establishes an uniform bound for $\|\sum_{i=k_1+1}^{k_2} \mathbf{U}_i\|$.

Lemma S.4 *Suppose Assumption 1 holds. Then we have as $n \rightarrow \infty$,*

$$\Pr \left(\max_{(k_1, k_2) \in \mathcal{T}(l, n)} (k_2 - k_1)^{-1} \left\| \sum_{i=k_1+1}^{k_2} \mathbf{U}_i \right\|^2 > C \log n \right) = O(n^{1-\alpha});$$

for some large $C > 0$ and any $0 < \alpha < 2^{-1}$.

Proof. We shall show that the assertion holds when $d = 1$ and the case for $d > 1$ is straightforward by using the Bonferroni inequality. Denote $M_n = n^{1-\alpha}$ for some $0 < \alpha < 1/2$, and observe that

$$\begin{aligned} U_i &= [U_i \mathbb{I}(|U_i| \leq M_n) - \mathbb{E}\{U_i \mathbb{I}(|U_i| \leq M_n)\}] + [U_i \mathbb{I}(|U_i| > M_n) - \mathbb{E}\{U_i \mathbb{I}(|U_i| > M_n)\}] \\ &=: U_{i1} + U_{i2}. \end{aligned}$$

It suffices to prove that the assertion holds with U_{i1} and U_{i2} respectively. Let $x = \sqrt{C \log n}$ with a sufficiently large C ,

$$\begin{aligned} &\Pr \left(\max_{(k_1, k_2) \in \mathcal{T}(l, n)} (k_2 - k_1)^{-1} \left(\sum_{i=k_1+1}^{k_2} U_i \right)^2 > x^2 \right) \\ &\leq \Pr \left(\max_{(k_1, k_2) \in \mathcal{T}(l, n)} (k_2 - k_1)^{-1/2} \left| \sum_{i=k_1+1}^{k_2} U_{i1} \right| > x/2 \right) \\ &\quad + \Pr \left(\max_{(k_1, k_2) \in \mathcal{T}(l, n)} (k_2 - k_1)^{-1/2} \left| \sum_{i=k_1+1}^{k_2} U_{i2} \right| > x/2 \right) \\ &=: P_1 + P_2. \end{aligned}$$

On one hand, by the Bernstein inequality in Lemma S.2, we have

$$P_1 \leq n^2 \Pr \left((k_2 - k_1)^{-1/2} \left| \sum_{i=k_1+1}^{k_2} U_{i1} \right| > x/2 \right) \leq 2n^2 \exp \left\{ -\frac{W_n x^2}{C_1 W_n + C_2 M_n W_n^{1/2} x} \right\} = o(n^{1-\alpha});$$

where C_1, C_2 are some positive constants and we use the assumption that $\epsilon < -2^{-1}$.

On the other hand, according to Cauchy inequality and Markov inequality, we note that

$$\mathbb{E}^2\{|U_i|\mathbb{I}(|U_i| > M_n)\} \leq \mathbb{E}(U_i^2) \Pr(|U_i| > M_n) \leq C_3 n^{-\epsilon};$$

for some constant $C_3 > 0$. Further, it yields $\max_{(k_1, k_2) \in \mathcal{T}(l, n)} (k_2 - k_1)^{1-2\epsilon} \mathbb{E}\{|U_i|\mathbb{I}(|U_i| > M_n)\} = o(1)$: Thus, by Assumption 1 and Markov inequality, we have

$$\begin{aligned} P_2 &\leq \Pr\left(\max_{(k_1, k_2) \in \mathcal{T}(l, n)} (k_2 - k_1)^{-1-2\epsilon} \sum_{i=k_1+1}^{k_2} |U_i|\mathbb{I}(|U_i| > M_n) > \epsilon\right) \\ &\leq \Pr\left(\max_{(k_1, k_2) \in \mathcal{T}(l, n)} (k_2 - k_1)^{-1-2\epsilon} \sum_{i=k_1+1}^{k_2} |U_i| > \epsilon \mid \max_i |U_i| > M_n\right) \Pr\left(\max_i |U_i| > M_n\right) \\ &\leq n \Pr(|U_i| > M_n) \leq C_4 n^{1-\epsilon}; \end{aligned}$$

for some positive constant C_4 . The lemma is proved.

A direct corollary of Lemma S.4 is the following lemma. Denote $\mathbf{T}_{1j} = \sqrt{\frac{n_j n_{j+1}}{n_j + n_{j+1}}} (n(\bar{\mathbf{S}}_j^O - \bar{\mathbf{S}}_{j+1}^O))$ and $\mathbf{T}_{2j} = \sqrt{\frac{n_j n_{j+1}}{n_j + n_{j+1}}} (\bar{\mathbf{S}}_j^E - \bar{\mathbf{S}}_{j+1}^E)$.

Lemma S.5 *Suppose Assumptions 1-2 hold. For those $j \in \mathcal{I}_0$, then we have as $n \rightarrow \infty$,*

$$\Pr\{\|\mathbf{T}_{kj}\|^2 > C(\log n + \frac{1}{n} \frac{2}{n})\} = O(n^{1-\epsilon}); \quad k = 1, 2$$

for some large $C > 0$ and any $0 < \epsilon < -2^{-1}$.

Proof. We take \mathbf{T}_{2j} as example. By Assumption 2, if there exists a true change point k^* between \hat{j}_{-1} and \hat{j}_{+1} , it can only be either close to \hat{j}_{-1} or \hat{j}_{+1} , but not \hat{j} . Without loss

of generality, assume $0 \leq k^* - \hat{j}_{-1} \leq n$. Then we note that

$$\begin{aligned}
\|\mathbf{T}_{2j}\| &= \left\| \sqrt{\frac{n_j n_{j+1}}{n_j + n_{j+1}}} \left\{ \frac{1}{n_j} \sum_{i=\hat{j}_{-1}+1}^{\hat{j}} \mathbf{v}_i - \frac{1}{n_{j+1}} \sum_{i=\hat{j}+1}^{\hat{j}+1} \mathbf{v}_i + \frac{k^* - \hat{j}_{-1}}{n_j} (\boldsymbol{\mu}_k^* - \boldsymbol{\mu}_{k+1}^*) \right\} \right\| \\
&\leq \sqrt{\frac{n_j}{n_j + n_{j+1}}} \left\| n_j^{-1/2} \sum_{i=\hat{j}_{-1}+1}^{\hat{j}} \mathbf{v}_i \right\| + \sqrt{\frac{n_{j+1}}{n_j + n_{j+1}}} \left\| n_{j+1}^{-1/2} \sum_{i=\hat{j}+1}^{\hat{j}+1} \mathbf{v}_i \right\| + \left\| \frac{k^* - \hat{j}_{-1}}{n_j} (\boldsymbol{\mu}_k^* - \boldsymbol{\mu}_{k+1}^*) \right\| \\
&\leq \sqrt{\frac{n_j}{n_j + n_{j+1}}} \left\| n_j^{-1/2} \sum_{i=\hat{j}_{-1}+1}^{\hat{j}} \mathbf{v}_i \right\| + \sqrt{\frac{n_{j+1}}{n_j + n_{j+1}}} \left\| n_{j+1}^{-1/2} \sum_{i=\hat{j}+1}^{\hat{j}+1} \mathbf{v}_i \right\| + n^{-1/2} \|\boldsymbol{\mu}_k^* - \boldsymbol{\mu}_{k+1}^*\| \\
&\leq 2 \max_{(k_1, k_2) \in \mathcal{T}(n)} (k_2 - k_1)^{-1/2} \left\| \sum_{i=k_1+1}^{k_2} \mathbf{v}_i \right\| + n^{-1/2} \|\boldsymbol{\mu}_k^* - \boldsymbol{\mu}_{k+1}^*\|.
\end{aligned}$$

The assertion is immediately verified by using Lemma S.4.

Appendix D: Proof of Proposition 1

The proof of this proposition follows similarly to Theorem 2 in Barber et al. (2020) which shows that the Model-X knockoff selection procedure incurs an inflation of the false discovery rate that is proportional to the errors in estimating the distribution of each feature conditional on the remaining features. Fix $\epsilon > 0$ and for any threshold $t > 0$, define

$$R(t) = \frac{\sum_{j \in \mathcal{I}_0} \mathbb{I}(W_j \geq t; \Delta_j \leq \epsilon)}{1 + \sum_{j \in \mathcal{I}_0} \mathbb{I}(W_j \leq -t)}.$$

Consider the event that $\mathcal{A} = \{\Delta := \max_{j \in \mathcal{I}_0} \Delta_j \leq \epsilon\}$. Furthermore, for a threshold rule

It is crucial to get an upper bound for $\mathbb{E}\{R(L) \mid \mathcal{Z}_O\}$. In what follows, all the “ $\mathbb{E}(\cdot)$ ” denote the expectations given \mathcal{Z}_O . We have

$$\begin{aligned}
\mathbb{E}\{R(L)\} &= \sum_{j \in \mathcal{I}_0} \mathbb{E} \left\{ \frac{\mathbb{I}(W_j \geq L; \Delta_j \leq \cdot)}{1 + \sum_{j \in \mathcal{I}_0} \mathbb{I}(W_j \leq -L)} \right\} \\
&= \sum_{j \in \mathcal{I}_0} \mathbb{E} \left\{ \frac{\mathbb{I}(W_j \geq L_j; \Delta_j \leq \cdot)}{1 + \sum_{k \in \mathcal{I}_0; k \neq j} \mathbb{I}(W_k \leq -L_j)} \right\} \\
&= \sum_{j \in \mathcal{I}_0} \mathbb{E} \left[\mathbb{E} \left\{ \frac{\mathbb{I}(W_j \geq L_j; \Delta_j \leq \cdot)}{1 + \sum_{k \in \mathcal{I}_0; k \neq j} \mathbb{I}(W_k \leq -L_j)} \mid |W_j|; \mathbf{W}_{-j} \right\} \right] \\
&= \sum_{j \in \mathcal{I}_0} \mathbb{E} \left\{ \frac{\Pr(W_j > 0 \mid |W_j|; W_{j-1}; W_{j+1}; \mathcal{Z}_O) \mathbb{I}(|W_j| \geq L_j; \Delta_j \leq \cdot)}{1 + \sum_{k \in \mathcal{I}_0; k \neq j} \mathbb{I}(W_k \leq -L_j)} \right\}; \quad (\text{S.1})
\end{aligned}$$

where the last step holds since the only unknown is the sign of W_j after conditioning on $(|W_j|; W_{j-1}; W_{j+1})$. By definition of Δ_j , we have $\Pr(W_j > 0 \mid |W_j|; W_{j-1}; W_{j+1}; \mathcal{Z}_O) \leq 1 - 2\Delta_j$.

Hence,

$$\begin{aligned}
\mathbb{E}\{R(L)\} &\leq \sum_{j \in \mathcal{I}_0} \mathbb{E} \left\{ \frac{(\frac{1}{2} + \Delta_j) \mathbb{I}(|W_j| \geq L_j; \Delta_j \leq \cdot)}{1 + \sum_{k \in \mathcal{I}_0; k \neq j} \mathbb{I}(W_k \leq -L_j)} \right\} \\
&\leq \left(\frac{1}{2} + \cdot\right) \left[\sum_{j \in \mathcal{I}_0} \mathbb{E} \left\{ \frac{\mathbb{I}(W_j \geq L_j; \Delta_j \leq \cdot)}{1 + \sum_{k \in \mathcal{I}_0; k \neq j} \mathbb{I}(W_k \leq -L_j)} \right\} + \sum_{j \in \mathcal{I}_0} \mathbb{E} \left\{ \frac{\mathbb{I}(W_j \leq -L_j)}{1 + \sum_{k \in \mathcal{I}_0; k \neq j} \mathbb{I}(W_k \leq -L_j)} \right\} \right] \\
&= \left(\frac{1}{2} + \cdot\right) \left[\mathbb{E}\{R(L)\} + \sum_{j \in \mathcal{I}_0} \mathbb{E} \left\{ \frac{\mathbb{I}(W_j \leq -L_j)}{1 + \sum_{k \in \mathcal{I}_0; k \neq j} \mathbb{I}(W_k \leq -L_j)} \right\} \right];
\end{aligned}$$

Finally, the sum in the last expression can be simplified as: if for all null j , $W_j > -L_j$, then the sum is equal to zero, while otherwise,

$$\sum_{j \in \mathcal{I}_0} \mathbb{E} \left\{ \frac{\mathbb{I}(W_j \leq -L_j)}{1 + \sum_{k \in \mathcal{I}_0; k \neq j} \mathbb{I}(W_k \leq -L_j)} \right\} = \sum_{j \in \mathcal{I}_0} \mathbb{E} \left\{ \frac{\mathbb{I}(W_j \leq -L_j)}{1 + \sum_{k \in \mathcal{I}_0; k \neq j} \mathbb{I}(W_k \leq -L_k)} \right\} = 1;$$

where the first step comes from the fact: for any $j; k$, if $W_j \leq -\min(L_j; L_k)$ and $W_k \leq -\min(L_j; L_k)$, then $L_j = L_k$; see Barber et al. (2020).

Accordingly, we have

$$\mathbb{E}\{R(L)\} \leq \frac{1+2}{1-2} \leq 1+5 :$$

Consequently, the assertion of this proposition holds.

Appendix E: Proof of Lemmas A.1-A.2

Note that both the candidate change-points set $\widehat{\mathcal{T}}_{\rho_n}$ and the statistics W_j are dependent with \mathcal{Z}_O . In fact, we derive the following two lemmas on the basis of conditional probability on \mathcal{Z}_O . To be specific, conditional on \mathcal{Z}_O , $\widehat{\mathcal{T}}_{\rho_n}$ is fixed as well as $(\bar{\mathbf{S}}_j^O - \bar{\mathbf{S}}_{j+1}^O)^\top$. Due to the independence between \mathcal{Z}_E and \mathcal{Z}_O , the standard results for independent sum such as Lemmas S.2-S.3 can be applied for $\bar{\mathbf{S}}_j^E - \bar{\mathbf{S}}_{j+1}^E$ in the following arguments.

Proof of Lemma A.1

Define $\rho_n = \{C(\log n + \frac{1}{n})\}^{1-2}$ for a large $C > 0$ specified in Lemma S.5. Let $\mathcal{A}_n = \{\mathbf{u} \in \mathbb{R}^d : \|\mathbf{u}\| \geq t = \rho_n\}$. Then, we observe that

$$\frac{G(t)}{G_-(t)} - 1 = \frac{\sum_{j \in \mathcal{I}_0} \{\Pr(\mathbf{T}_{1j}^\top \mathbf{T}_{2j} \geq t \mid \mathcal{Z}_O) - \Pr(\mathbf{T}_{1j}^\top \mathbf{T}_{2j} \leq -t \mid \mathcal{Z}_O)\}}{\rho_0 G_-(t)}$$

Conditional on \mathcal{Z}_O , we have two cases. Firstly, for the case $\mathbf{T}_{1j} \in \mathcal{A}_n^c$, by Lemma S.5 we obtain that

$$\frac{G(t)}{G_-(t)} - 1 \leq \frac{\sum_{j \in \mathcal{I}_0} \Pr(\mathbf{T}_{1j}^\top \mathbf{T}_{2j} \geq t \mid \mathcal{Z}_O)}{\rho_0 G_-(t)} \leq \frac{\sum_{j \in \mathcal{I}_0} \Pr(\|\mathbf{T}_{2j}\| > \rho_n \mid \mathcal{Z}_O)}{\rho_0 = \rho_n} = O_p(n^{1-\rho_n});$$

where the first inequality is due to $t \leq G_-^{-1}(1-\rho_n)$, and thus we claim that $\frac{G(t)}{G_-(t)} - 1 = O_p(n^{1-\rho_n})$.

Next, we consider the case $\mathbf{T}_{1j} \in \mathcal{A}_n$. We introduce a new sequence of independent random variables $\{\mathbf{B}_i\}$ defined as follows:

$$\mathbf{B}_i = \begin{cases} \frac{\sqrt{n_j n_{j+1}}}{n_j \sqrt{n_j + n_{j+1}}} \mathbf{V}_i; & \widehat{j}_{-1} < i \leq \widehat{j}; \\ -\frac{\sqrt{n_j n_{j+1}}}{n_{j+1} \sqrt{n_j + n_{j+1}}} \mathbf{V}_i; & \widehat{j} < i \leq \widehat{j}_{+1}. \end{cases}$$

By Lemma S.3, we firstly verify that for any given $\mathbf{u} \in \mathcal{A}_n$,

$$\frac{\Pr \left\{ \sum_{i=\hat{j}-1+1}^{\hat{j}+1} \mathbf{u}^\top \mathbf{B}_i \geq t \mid \mathcal{Z}_O \right\}}{1 - \Phi(t=\sqrt{\quad})}$$

Proof of Lemma A.2

We only show the validity of the first formula and the second one hold similarly. Note that the $G(t)$ is a decreasing and continuous function. Let $z_0 < z_1 < \dots < z_{d_n} \leq 1$ and $t_i = G^{-1}(z_i)$, where $z_0 = a_n - \rho_n$; $z_i = a_n - \rho_n + a_n i^{-\rho_n}$; $d_n = \lceil \{(a_n - \rho_n) - a_n\}^{-1/\rho_n} \rceil$ with $\rho_n > 1$. Note that $G(t_i) = G(t_{i+1}) = 1 + o(1)$ uniformly in i . It is therefore enough to obtain the convergence rate of

$$D_n = \sup_{0 \leq i \leq d_n} \left| \frac{\sum_{j \in \mathcal{I}_0} \{\mathbb{I}(W_j \geq t_i) - \Pr(W_j \geq t_i | \mathcal{Z}_O)\}}{\rho_0 G(t_i)} \right|.$$

Define $\mathcal{S}_j = \{k \in \mathcal{I}_0 : W_k \text{ is dependent with } W_j\}$ and further

$$D(t) = \mathbb{E} \left[\left\{ \sum_{j \in \mathcal{I}_0} \mathbb{I}(W_j \geq t) - \Pr(W_j \geq t | \mathcal{Z}_O) \right\}^2 \mid \mathcal{Z}_O \right].$$

It is noted that

$$D(t) = \sum_{j \in \mathcal{I}_0} \sum_{k \in \mathcal{S}_j} \mathbb{E} [\{\mathbb{I}(W_j \geq t) - \Pr(W_j \geq t | \mathcal{Z}_O)\} \{\mathbb{I}(W_k \geq t) - \Pr(W_k \geq t | \mathcal{Z}_O)\} \mid \mathcal{Z}_O] \leq 2\rho_0 G(t):$$

Note that conditional on \mathcal{Z}_O , W_1, \dots, W_{ρ_n} is a 1-dependent sequence and so is $\mathbb{I}(W_j \geq t_i)$.

We can get

$$\begin{aligned} \Pr(D_n \geq \epsilon) &\leq \sum_{i=0}^{d_n} \Pr \left(\left| \frac{\sum_{j \in \mathcal{I}_0} \{\mathbb{I}(W_j \geq t_i) - \Pr(W_j \geq t_i | \mathcal{Z}_O)\}}{\rho_0 G(t_i)} \right| \geq \epsilon \right) \\ &\leq \frac{1}{2} \sum_{i=0}^{d_n} \frac{1}{\rho_0^2 G^2(t_i)} D(t_i) \leq \frac{2}{2} \sum_{i=0}^{d_n} \frac{1}{\rho_0 G(t_i)}. \end{aligned}$$

Moreover, observe that

$$\begin{aligned} \sum_{i=0}^{d_n} \frac{1}{\rho_0 G(t_i)} &= \frac{\rho_n}{\rho_0} \left(\frac{1}{a_n} + \sum_{i=1}^{d_n} \frac{1}{a_n + a_n i} \right) \\ &\leq c \left(\frac{1}{a_n} + a_n^{-1} \sum_{i=1}^{d_n} \frac{1}{1+i} \right) \leq c a_n^{-1} \{1 + O(1)\}. \end{aligned}$$

In sum, we can have $\Pr(D_n \geq \epsilon) \rightarrow 0$ provided that $a_n \rightarrow \infty$.

Appendix F: Proof of Theorems 1-3 and Corollaries 1-2

Proof of Corollary 1

(i) By Assumption 2, we know that the event that $|\mathcal{I}_1| = K_n$ and for each $\hat{j} \in \mathcal{I}_1$, $|\hat{j} - j^*| \leq \frac{1}{n}$ occur with probability approaching one as $n \rightarrow \infty$. Therefore, in what follows we always implicitly work with the occurrence of this event. From the proof of Theorem 1, we know that $L \leq \frac{2}{n}$. Hence

$$\begin{aligned}
& \Pr(W_j < L; \text{ for some } \hat{j} \in \mathcal{I}_1 \mid \mathcal{Z}_O) \\
& \leq K_n \Pr\left(\frac{\eta_j \eta_{j+1}}{\eta_j + \eta_{j+1}} (\bar{\mathbf{S}}_j^O - \bar{\mathbf{S}}_{j+1}^O)^\top \quad n(\bar{\mathbf{S}}_j^E - \bar{\mathbf{S}}_{j+1}^E) < L \mid \mathcal{Z}_O\right) \\
& \leq K_n \Pr\left(\frac{\eta_j \eta_{j+1}}{\eta_j + \eta_{j+1}} (\bar{\mathbf{U}}_j - \bar{\mathbf{U}}_{j+1})^\top \quad n(\bar{\mathbf{V}}_j - \bar{\mathbf{V}}_{j+1}) + O_\rho^+(\frac{1}{n} \min_{1 \leq k \leq K_n} \|\boldsymbol{\mu}_{k+1}^* - \boldsymbol{\mu}_k^*\|^2) < L \mid \mathcal{Z}_O\right) \\
& \leq K_n \Pr\left(O_\rho^+(\frac{1}{n} \min_{1 \leq k \leq K_n} \|\boldsymbol{\mu}_{k+1}^* - \boldsymbol{\mu}_k^*\|^2) \leq L\right) \\
& \quad + K_n \Pr\left(\frac{\eta_j \eta_{j+1}}{\eta_j + \eta_{j+1}} (\bar{\mathbf{U}}_j - \bar{\mathbf{U}}_{j+1})^\top \quad n(\bar{\mathbf{V}}_j - \bar{\mathbf{V}}_{j+1}) > O_\rho^+(\frac{1}{n} \min_{1 \leq k \leq K_n} \|\boldsymbol{\mu}_{k+1}^* - \boldsymbol{\mu}_k^*\|^2) \mid \mathcal{Z}_O\right) \rightarrow 0
\end{aligned}$$

in probability, where we use Lemma S.4. The result immediately holds.

(ii) From (i), we have $\lim_{n \rightarrow \infty} \Pr(\mathcal{M} \supseteq \mathcal{I}_1) = 1$. Here, we only need to prove $\lim_{n \rightarrow \infty} \Pr(\mathcal{M} \subseteq \mathcal{I}_1) = 1$, which is equivalent to show that $\lim_{n \rightarrow \infty} \Pr(\mathcal{M} \cap \mathcal{I}_0 = \emptyset) = 1$.

It is noted that

$$\Pr(W_j \geq L; \text{ for some } j \in \mathcal{I}_0 \mid \mathcal{Z}_O) \leq \sum_{j \in \mathcal{I}_0} \Pr(W_j \geq L \mid \mathcal{Z}_O) \sim \rho_0 \frac{n}{\rho_n} \cdot K_n ;$$

By using the condition $K_n \rightarrow 0$, the corollary is proved.

Proof of Theorem 1

Following the notations in Section 2, assume $\hat{j} \in \mathcal{M}$ is an informative point and j^* is its corresponding true change-point such that $|\hat{j} - j^*| \leq \frac{1}{n}$ by Assumption 2. Note that $\tilde{k} \in \tilde{\mathcal{M}}$ is the selected one such that $|\tilde{k} - \hat{j}| = \min_{l \in \tilde{\mathcal{M}}} |\tilde{l} - \hat{j}|$. Because \mathcal{M} and $\tilde{\mathcal{M}}$ have

the same cardinality, we only need to show that $\tilde{k} \in \mathcal{I}_1(\tilde{\mathcal{T}}_{p_n})$, say

$$|\tilde{k} - j^*| = \min_{\tilde{l} \in \tilde{\mathcal{T}}_{p_n}} |\tilde{l} - j^*| \quad (\text{S.2})$$

(ii) Let $a_n = (C \log n)^{1=2}$, where $C > 0$ is specified in Lemma S.5. Define $\mathcal{B}_n = \{\mathbf{u} \in \mathbb{R}^d : \|\mathbf{u}\| \geq t=a_n\}$. Let $\mathcal{C} = \bigcap_{j \in \mathcal{I}_0} \{|\tilde{W}_j| \leq j\}$, where j satisfies $\Pr(|\tilde{W}_j| > j \mid \mathcal{Z}_O) = b_n$ and b_n be a sequence satisfies the conditions that $b_n \rightarrow 0$, $\rho_n b_n \rightarrow 0$ and $n^{-2} b_n \rightarrow \infty$. According to the condition $\rho_n n^{-2} \rightarrow 0$ in the theorem, such b_n is well defined. By the definition of \tilde{W}_j , we know that $\mathbb{E}(\tilde{W}_j) = 0$ for all $j \in \mathcal{I}_0$. Moreover, by Lemma S.5, we have $j \cdot a_n^2$ uniformly in j .

According to Proposition 1, we have

$$\begin{aligned} \Pr\left(\max_{j \in \mathcal{I}_0} \Delta_j > \mid \mathcal{Z}_O\right) &= \Pr\left(\max_{j \in \mathcal{I}_0} \Delta_j > \mid \mathcal{C}; \mathcal{Z}_O\right) \Pr(\mathcal{C} \mid \mathcal{Z}_O) + \Pr\left(\max_{j \in \mathcal{I}_0} \Delta_j > ; \mathcal{C}^c \mid \mathcal{Z}_O\right) \\ &\leq \Pr\left(\max_{j \in \mathcal{I}_0} \Delta_j > \mid \mathcal{C}; \mathcal{Z}_O\right) + \Pr(\mathcal{C}^c \mid \mathcal{Z}_O) := A_1 + A_2: \end{aligned}$$

By the definition of b_n , $A_2 = o_p(1)$. It remains to handle A_1 .

Notice that conditional on \mathcal{C} ,

$$\max_{j \in \mathcal{I}_0} \Delta_j \leq \max_{j \in \mathcal{I}_0} \sup_{0 \leq t \leq j} |f_j(-t) - f_j(t) - 1|; \quad (\text{S.3})$$

where $f_j(\cdot)$ is the density of \tilde{W}_j conditional on \mathcal{Z}_O . It remains to prove that the right-hand side of (S.3) goes to zero as $n \rightarrow \infty$.

Denote $\tilde{\mathbf{T}}_{1j} = \sqrt{\frac{n_j n_{j+1}}{n_j + n_{j+1}}} (n(\tilde{\mathbf{S}}_{Lj}^O - \tilde{\mathbf{S}}_{Rj}^O) = \mathbf{u}$ given \mathcal{Z}_O . In a similar way to the proof of Lemma A.1, we consider two cases for \mathbf{u} . As to the case $\mathbf{u} \in \mathcal{B}_n^c$, $\max_{j \in \mathcal{I}_0} \Delta_j = O_p\{(n^{-2} b_n)^{-1}\}$ by the definition of j and $0 \leq t \leq j$. On the other hand, we consider the case $\mathbf{u} \in \mathcal{B}_n$. Then, for $j \in \mathcal{I}_0$ by Lemma S.3, we have

$$f_j(t) = \{\tilde{\Phi}(t=s) - \tilde{\Phi}(t=s-)\} \{1 + o_p(1)\} = \frac{1}{s} (t=s) \{1 + o_p(1)\};$$

where $s = \sqrt{\mathbf{u}^\top \mathbf{u}}$. Similarly, we also have $f_j(-t) = \frac{1}{s} (-t=s) \{1 + o_p(1)\}$, which yields that the right-hand side of (S.3) goes to zero since $(-t=s) = (t=s)$ and $(t=s)$ is bounded. Then, the result (ii) in the theorem holds.

Appendix G: Additional simulation results

Selection of ρ_n and $!_n$

Table S1 reports the FDR, TPR and \widehat{K} of MOPS in conjunction with OP, PELT and WBS detection algorithms with different ρ_n and $!_n$ under Example I. We consider the error from $N(0;1)$ and fix $n = 4096$, $K_n = 15$ and $\text{SNR}=0.5$. We observe that different values of $c \in (1;2]$ for $\rho_n = \lfloor cn^{2=5} \rfloor$ and $\in [0.3;0.5]$ for $!_n = n$ present similar results and their FDRs are not significantly different. Thus we recommend $\rho_n = \lfloor 2n^{2=5} \rfloor$ and $!_n = \min(\lfloor n^{0.5} \rfloor; 60)$ in the simulation studies.

Table S1: *FDR(%), TPR(%) and \widehat{K} of MOPS in conjunction with OP, PELT and WBS detection algorithms when error follows $N(0;1)$, $n = 4096$, $K_n = 15$ and $\text{SNR}=0.5$ under Example I. The ρ_n is chosen as $\rho_n = \lfloor cn^{2=5} \rfloor$ with $c = 1.2;1.5;2$ and $!_n = n$ with $\in [0.3;0.4;0.5]$.*

ρ_n	Method	$\in [0.3$			$= 0.4$			$= 0.5$		
		FDR	TPR	\widehat{K}	FDR	TPR	\widehat{K}	FDR	TPR	\widehat{K}
$1.2n^{2=5}$	M-OP	19.8	91.3	17.7	19.1	92.7	17.9	18.9	95.2	18.3
	M-PELT	19.5	91.2	17.5	19.4	93.1	18.0	19.9	95.7	18.8
	M-WBS	16.9	91.8	17.3	17.2	92.3	17.5	19.5	95.3	18.5
$1.5n^{2=5}$	M-OP	18.6	90.0	17.2	21.0	92.9	18.6	20.5	93.7	18.4
	M-PELT	16.6	89.3	16.7	20.8	93.1	18.6	21.2	94.1	18.9
	M-WBS	17.3	85.9	16.3	18.3	86.3	16.6	16.4	90.9	17.0
$2n^{2=5}$	M-OP	20.5	79.5	17.4	19.5	82.1	16.5	20.4	85.3	17.0
	M-PELT	20.2	80.3	17.1	20.0	82.7	16.7	19.7	85.5	17.0
	M-WBS	19.6	76.7	15.9	17.8	77.8	15.8	18.1	83.1	16.5

Next, we investigate the performance of our methods in the case that $\rho_n > 2n^{2=5}$. Figure S1 presents the FDR and TPR curves of MOPS, R-MOPS and M-MOPS when ρ_n varies in $(2n^{2=5}; n=10)$ and the WBS algorithm is employed under Example I. Here we fix $!_n = 10$ and the true change-point number $K_n = 30$ and consider the error comes from $N(0;1)$ and standardized $\chi^2(3)$. The FDR values of MOPS vary in an acceptable range of the target level

no matter the choice of ρ_n under normal error, but are slightly distorted under standardized $\chi^2(3)$ error. The R-MOPS is able to improve TPR and yield smaller FDR levels than MOPS due to the use of full sample information. We also observe that the M-MOPS leads to more conservative FDR levels and smaller TPR than R-MOPS because of only using half of the observations around each candidate point. That is consistent with our theoretical analysis in Proposition 1 and Theorem 3. Similar results can also be found in Figure S2.

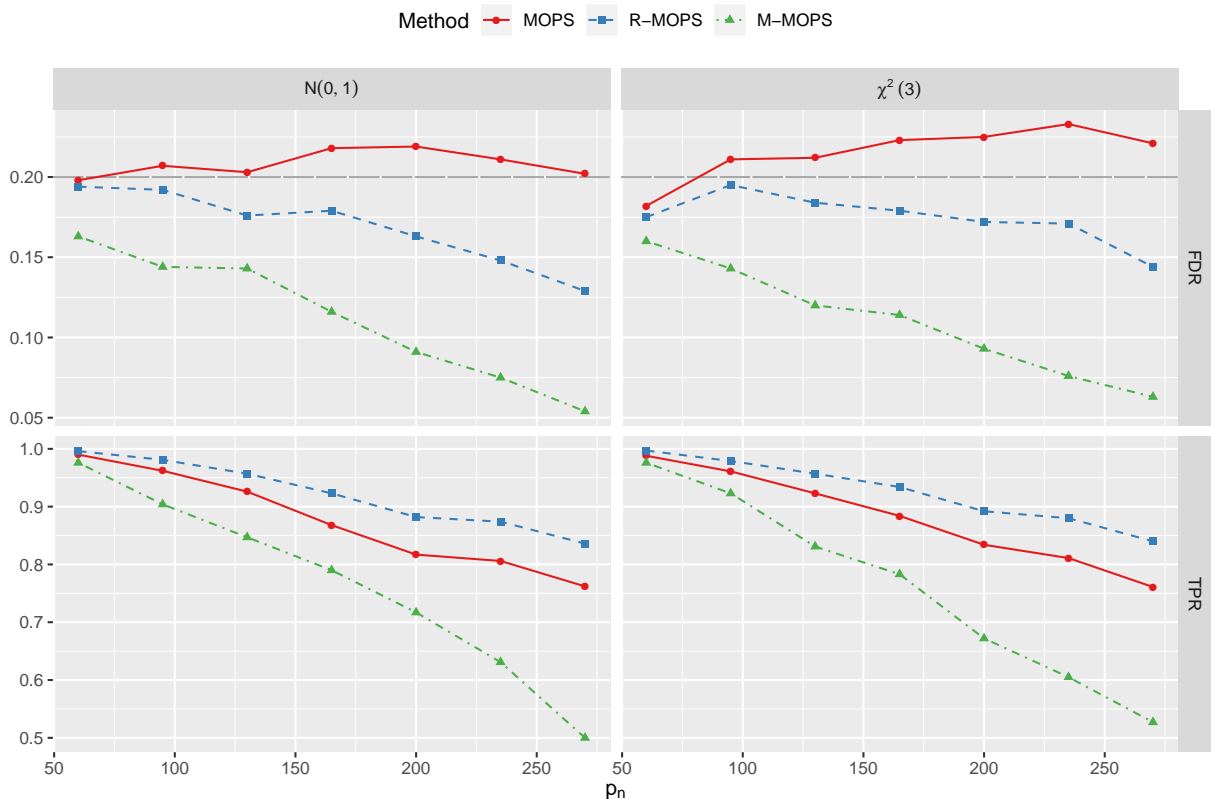


Figure S1: FDR and TPR curves against $\rho_n \in (2n^{2=5}; n=10)$ of MOPS, R-MOPS and M-MOPS in conjunction with WBS algorithm when $n = 4096$, $K_n = 30$ and $SNR=1$ under Example I. The $!_n$ is fixed as 10.

Figure S2 shows the FDR and TPR curves against $!_n$ of the MOPS, R-MOPS and M-MOPS in conjunction with WBS algorithm when $n = 4096$, $K_n = 10$ and ρ_n is fixed as $\lfloor 2n^{2=5} \rfloor$ under Example I. It implies that all the procedures are not sensitive to the choice of $!_n$ in terms of FDR control. Meanwhile, a large $!_n$ could improve the detection power due

to more observations in each segment.

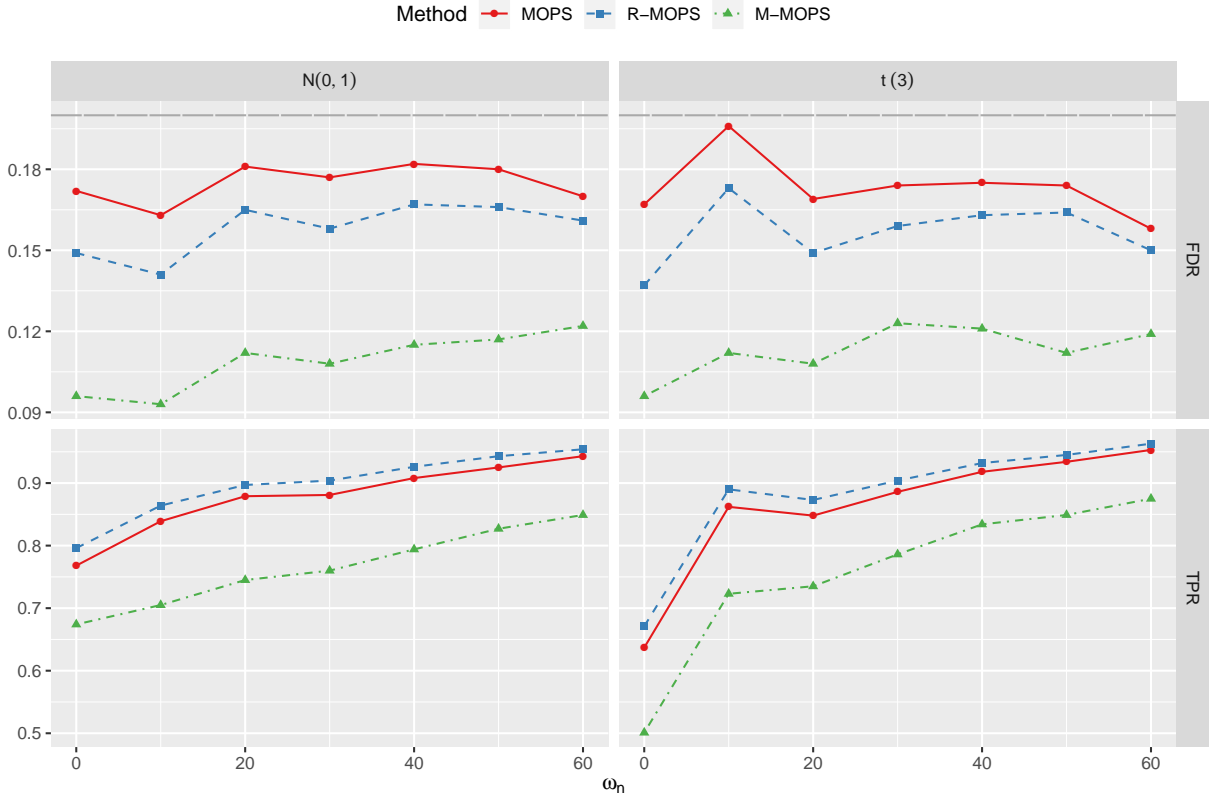


Figure S2: *FDR and TPR curves against ω_n of MOPS, R-MOPS and M-MOPS in conjunction with WBS algorithm when $n = 4096$, $K_n = 10$ and $SNR=0.7$ under Example I. The p_n is fixed as $\lfloor 2n^{2=5} \rfloor$.*

Comparison under other models

Three other MCP models are considered, reflecting changes in different aspects such as the location and scale. Table S2 gives a summary of all three simulated models along with the associated statistics \bar{S}_j^O in constructing W_j .

Under multivariate mean change model (Example III), we examine the performance of the refined MOPS in conjunction with the OP and PELT algorithms. For simplicity, each dimension of the signals μ_j 's is set as the same as the signals μ_j 's in Example I. Two scenarios for the error distribution are considered: (i) $\epsilon_j \stackrel{iid}{\sim} N(\mathbf{0}; \Sigma)$ with $\Sigma = (0.5^{|i-j|})_{d \times d}$;

Table S2: Preview of simulated models and the sample mean \mathbf{S}_j^O of the j -th segment for the odd part. Change-points $\hat{\tau}_j$'s are estimated on the basis of \mathcal{Z}_O .

NO.	Model	\mathbf{S}_j^O
III	$\mathbf{X}_i = \boldsymbol{\mu}_i + \boldsymbol{\varepsilon}_i$	$\mathbf{X}_{j-1:\hat{\tau}_j}^O$
IV	$\mathbf{X}_i \sim \text{Multinomial}(m; \mathbf{q}_i)$	$\mathbf{X}_{j-1:\hat{\tau}_j}^O$
V	$X_i = \mu_{ij}$	$V_{j-1:\hat{\tau}_j}^O, V_i = \log X_i^2$

(ii) $\boldsymbol{\varepsilon}_i = (\varepsilon_{i1}; \dots; \varepsilon_{id})^\top$, where $\varepsilon_{i1}; \dots; \varepsilon_{id} \stackrel{\text{iid}}{\sim} (\frac{2}{5} - 5) = \sqrt{10}$. We consider the dimension $d = 5$, 10 and adjust the scale parameter to $\sigma = 9\sqrt{d}$. Table S3 presents the results when the sample size $n = 3072$ and the number of change-points $K_n = 27$. The R-MOPS-based methods perform reasonably well in terms of FDR control and reliable TPR. In contrast, the CV-PELT results in overly conservative FDR levels across all the settings and its P_a 's are much smaller than those of R-MOPS.

Table S3: Comparison results of FDR(%), TPR(%), P_a (%) and \hat{K} when $K_n = 27$ and $n = 3072$ under Example III (multivariate mean shift).

errors	Method	$d = 5$				$d = 10$			
		FDR	TPR	P_a	\hat{K}	FDR	TPR	P_a	\hat{K}
$\boldsymbol{\varepsilon}_i \sim N(0; \sigma)$	RM-OP	18.5	97.1	53.5	32.9	18.9	92.9	35.0	32.1
	RM-PELT	18.7	97.5	54.0	32.8	18.5	92.5	33.5	31.9
	CV-PELT	0.9	91.3	18.0	24.9	0.6	86.7	4.0	23.6
$\mu_{ij} \sim \frac{2-5}{\sqrt{10}}$	RM-OP	19.7	99.1	87.0	33.0	20.3	95.9	68.5	33.1
	RM-PELT	19.5	99.0	85.5	32.7	20.8	96.2	69.5	33.3
	CV-PELT	0.8	85.9	4.5	23.4	1.7	84.1	0.0	23.1

Further, we consider the MCP problem for multinomial distributions (Example IV), i.e. $\mathbf{X}_i \sim \text{Multinom}(\eta_0; \mathbf{q}_i)$, where the variance of the observation relies on their mean. Braun et al. (2000) integrated the problem into quasi-likelihood framework in combination with BIC to determine the number of change-points. In particular, they aimed to identify the

breaks in the probability vectors \mathbf{q}_i 's and recommended the BIC with a penalty $\rho_n = 0.5n^{0.23}$, which will be seen as a benchmark for comparison in this example. To implement MOPS, we apply their algorithm in our training step, i.e., given a candidate model size ρ_n , we obtain the estimated change-points by constructing the statistics W_j in (5). We follow the same mechanism in Braun et al. (2000) to generate \mathbf{q}_i 's. To be specific, the initial mean vector $\mathbf{q} = (q_1; \dots; q_d)^\top$ is given as $q_j = U_j = \sum_{l=1}^d U_l$ for $j = 1; \dots; d$ where $U_j \sim \text{Uniform}(0;1)$. The jump mean vector $\mathbf{q}_k^* = (q_1^*; \dots; q_d^*)^\top$ for change point k is obtained by normalizing $\text{expit}(\text{logit}q_l^* + U_l^*)$ for $l = 1; \dots; d$ where $U_l^* \sim \text{Uniform}(-J;J)$ with $J = 0.8\sqrt{d}$. Table S4 reports the simulation results when $n = 2048$, $K_n = 20$, $n_0 \in (80;100;120)$ and d is chosen as 5 or 10. Again, our R-MOPS can successfully control the FDR at the nominal level in most cases. The BIC method appears to result in a slightly underfitting model on average. Accordingly, the BIC method delivers conservative FDR levels and it may miss some change-points due to relatively low P_a .

Table S4: Comparison results of FDR(%), TPR(%), P_a (%) and \hat{K} between R-MOPS and BIC in conjunction with Braun et al. (2000)'s algorithm when $K_n = 20$ and $n = 2048$ under Example IV.

n_0	Method	$d = 5$				$d = 10$			
		FDR	TPR	P_a	\hat{K}	FDR	TPR	P_a	\hat{K}
80	R-MOPS	20.2	98.1	85.5	25.2	17.1	92.8	45.0	23.1
	BIC	1.8	92.2	41.0	19.4	1.9	89.2	32.0	19.3
100	R-MOPS	21.1	99.2	92.0	26.0	20.1	98.3	75.5	25.2
	BIC	1.6	94.7	62.5	19.6	1.5	93.2	55.5	19.5
120	R-MOPS	21.5	99.8	97.5	26.2	21.2	99.0	85.0	26.0
	BIC	1.3	97.2	73.5	19.7	1.1	96.4	69.0	19.6

At last, we investigate the performance of R-MOPS in conjunction with PELT under Example V when the scale signal function of y_t 's is chosen as a piecewise constant function with values alternating between 1 and 0.5. We fix $n = 4096$ and show the curves of FDR, TPR and P_a when $K_n \in [28;35]$ in Figure S3. We observe that the FDRs of R-MOPS

with PELT get closer to the target level as K_n increases, which is in accordance with the theoretical justification. Meanwhile, the CV-PELT method usually results in an underfitting model because some true change-points are not selected.

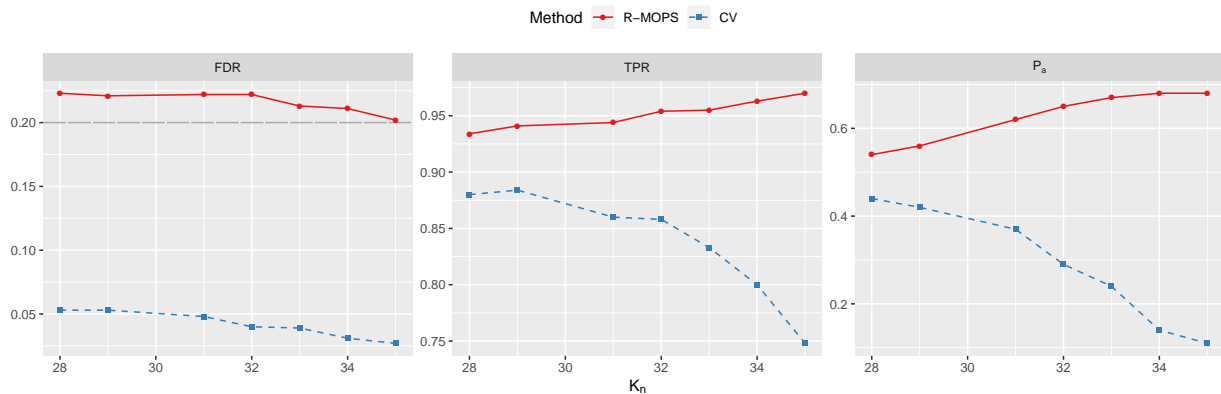


Figure S3: FDR , TPR and P_a curves against K_n between R -MOPS and CV criterion based on PELT when $n = 4096$ and errors are *i.i.d* from standardized t_5 under Example V.

Extension on controlling PFER

Table S5 reports some PFER results of the MOPS in conjunction with OP and PELT when the target PFER level $k_0 = 1/5$ or $1/10$. We fix the sample size $n = 4096$, the dimension $d = 5$ for multivariate data and consider that all errors are distributed from $\mathcal{N}(0; 1)$. The validity of our MOPS approach in terms of PFER control is clear.

Others

Figure S4 displays the performance comparison under Example I with the same model setting as Section 5.1 when the target FDR level is $\alpha = 0.1$. The comparison results are analogous to those in nominal level $\alpha = 0.2$.

Table S6 presents the comparisons between our R-SaRa and dFDR-SaRa under Example I. Following the recommendation in Hao et al. (2013), we choose four thresholds $h_1 = \lfloor 3 \log n \rfloor$, $h_2 = \lfloor 5 \log n \rfloor$, $h_3 = \lfloor 7 \log n \rfloor$ and $h_4 = \lfloor 9 \log n \rfloor$ as simple competitors. It is

Table S5: *PFER performance of MOPS in conjunction with OP and PELT when the target PFER level $k_0 = 1; 5$ and 10 under Examples I-V.*

Example	Method	k_0	$K_n = 5$			$K_n = 10$			$K_n = 15$		
			1	5	10	1	5	10	1	5	10
I	M-OP		1.08	5.07	9.83	0.98	5.13	9.73	0.92	4.96	10.56
	M-PELT		0.86	4.94	9.86	0.91	5.23	10.18	1.06	5.07	10.90
II	M-OP		0.79	4.86	10.03	0.69	4.72	10.25	0.89	4.97	10.04
	M-PELT		0.74	4.14	9.57	0.77	4.93	10.36	0.66	5.05	8.58
III	M-OP		0.65	5.04	10.05	1.06	5.10	10.13	0.94	5.01	10.72
	M-PELT		0.67	4.78	9.83	0.83	4.87	10.27	0.72	4.91	10.60
IV	M-OP		0.81	4.13	9.18	1.01	5.16	9.93	0.97	5.13	9.75
	M-PELT		0.68	4.22	9.00	1.02	4.74	9.74	0.83	5.09	10.08
V	M-OP		0.78	5.10	9.93	0.89	5.09	10.08	1.13	5.07	10.89
	M-PELT		0.62	4.97	10.21	0.77	4.89	10.38	0.72	5.02	11.12

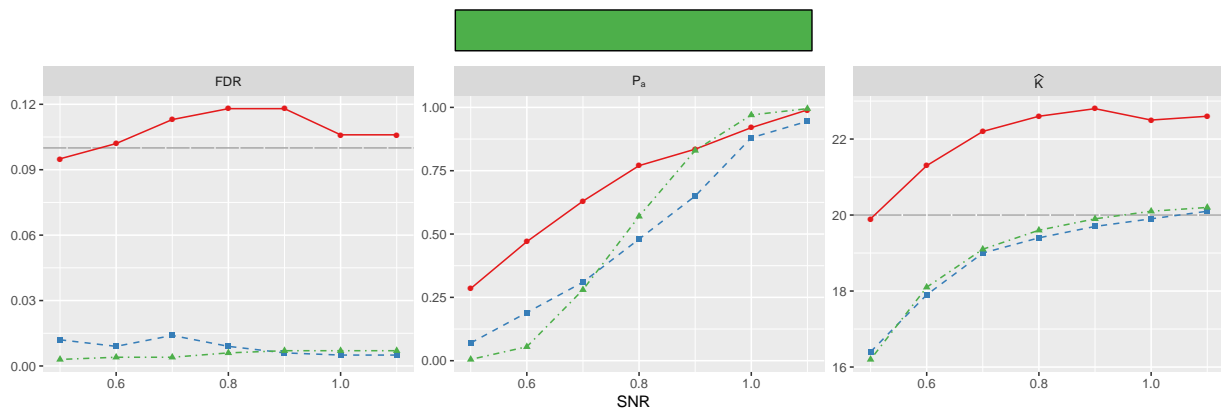


Figure S4: *FDR, P_a and the average number of estimated change-points \hat{K} curves against SNR among RM-PELT, CV-PELT and FDRseg when $K_n = 20$, $n = 2048$ and the target FDR level = 0:1 under Example I.*

clear that the R-MOPS performs well in terms of FDR control, but the performance of dFDR-SaRa depends on the choice of h to a large extent.

For the frequent change-point setting, Fryzlewicz (2020) proposed WBS2 detection algo-

Table S6: Comparison results of FDR(%), TPR(%), P_a (%) and \hat{K} between RM-Sara and dFDR-SaRa-h in Hao et al. (2013) when $n = 10240$ and $SNR=0.7$ under Example 1.

Errors	Method	$K_n = 20$				$K_n = 40$			
		FDR	TPR	P_a	\hat{K}	FDR	TPR	P_a	\hat{K}
$N(0;1)$	RM-SaRa	19.5	99.2	84.0	25.4	22.2	99.8	92.0	52.2
	dFDR-SaRa- h_1	17.1	78.2	6.5	19.2	10.7	83.9	1.0	37.8
	dFDR-SaRa- h_2	10.2	94.3	44.0	21.0	3.0	95.9	29.0	39.6
	dFDR-SaRa- h_3	9.6	97.3	70.5	21.6	0.2	98.3	49.5	39.4
	dFDR-SaRa- h_4	3.4	99.1	90.0	20.5	0.0	95.8	1.0	38.3
${}^2(3)$	RM-SaRa	18.6	99.7	94.5	25.3	20.9	99.9	96.5	51.1
	dFDR-SaRa- h_1	16.8	89.2	18.5	21.6	11.0	92.8	13.5	41.9
	dFDR-SaRa- h_2	12.8	98.1	74.0	22.7	2.0	99.3	81.0	40.5
	dFDR-SaRa- h_3	7.2	99.7	96.5	21.6	0.3	99.8	92.0	40.0
	dFDR-SaRa- h_4	2.6	100.0	100.0	20.6	0.0	95.3	0.0	39.0

rithm with threshold-based model selection criterion “Steepest Drop to Low Levels” (SDLL). We compare our procedure R-MOPS in conjunction with WBS2 to the WBS2.SDLL criterion when the “extreme.teeth” example of the univariate changes in Fryzlewicz (2020) is considered. Specially, in the “extreme.teeth” example, the mean μ_i 's for each observation are defined as follows: $\mu_i = 0$ if $1 \leq \text{mod}(i;10) \leq 5$ and $\mu_i = 1$ if $\text{mod}(i;10) \in \{0;6;7;8;9\}$, and the sample size n is 1000. Two values of SNR and three error distributions including $N(0;1)$, standardized $t(3)$ and standardized ${}^2(3)$ are considered. We fix $!_n = 4$ and $\rho_n = 250$ for the R-MOPS. From Table S7, we can see that the FDRs of R-MOPS with WBS2 are still controlled, though they appear to be overly conservative. The WBS2.SDLL generally has better performances in terms of \hat{K} estimation in the most settings.

Another real-data example: OPEC oil price

We analyze the daily Organisation of the Petroleum Exporting Countries (OPEC) Reference Basket oil prices from Jan. 6, 2003 to Dec. 16, 2020 with sample size $n = 4610$, which is available from <https://www.quandl.com>. As the raw oil price series tend to ex-

Table S7: Comparisons of \hat{K} , FDR(%) and TPR(%) between R-MOPS and SDLL in conjunction with WBS2 Fryzlewicz (2020)'s "extreme.teeth" example when $n = 1000$, $K_n = 199$ and three error distributions are considered. The target FDR level is $\alpha = 0.2$ and σ^2 is the error variance.

Error	Method	$\alpha = 0.3$			$\alpha = 0.5$		
		\hat{K}	FDR	TPR	\hat{K}	FDR	TPR
N(0;1)	RMOPS	193.7	7.1	90.4	160.6	10.0	72.6
	SDLL	199.4	3.8	96.4	71.6	9.0	29.3
t(3)	RMOPS	193.9	7.1	90.5	176.5	8.0	81.6
	SDLL	209.8	7.1	97.8	221.8	19.6	89.0
$\chi^2(3)$	RMOPS	193.1	7.1	90.2	167.9	8.9	76.8
	SDLL	211.0	8.1	97.2	200.5	22.8	77.3

hibit strong autocorrelation (Baranowski et al., 2019), we consider analyzing the log-returns $100 \log(P_i/P_{i-1})$, where P_i is the daily oil price. Figure S5 presents the data sequence of log-returns and its autocorrelation, indicating the correlations of log-returns are relatively weak. As Baranowski et al. (2019) pointed out that both mean and scale changes exist in the sequence, we build $\mathbf{S}_i = (\mathbb{Z}_i, \log(\mathbb{Z}_i^2))^\top$ in W_j for the proposed MOPS procedure to detect changes in both the mean and variance when PELT algorithm is applied. In this study, we use the function `cpt.meanvar()` in R package `changept` to implement the PELT algorithm and also report change-points detected by the BIC for comparison.

The BIC results in 33 change-points, while the R-MOPS with PELT yields 36 and 55 change-points when the target FDR level is 0.05 and 0.1, respectively. The locations of the change-points identified by BIC and R-MOPS with $\alpha = 0.05$ are given in the left panel of Figure S5. The estimated change-points of both methods largely agree each other. However, the BIC does not indicate any changes in late 2004 and early 2005 and meanwhile R-MOPS has several estimated change-points in that period. This period could potentially be related to a noticeable expansion of the production volume in the late 2004, which leads to a significant change of oil price elasticity. Thus, Murray and King (2012) called the early

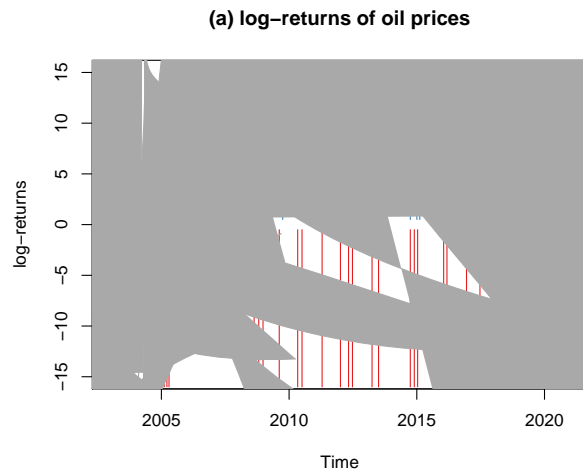


Figure S5: (a): Scatter plots of the log-returns of daily OPEC oil prices, where the blue dash and red solid lines represent the estimated change-points detected by BIC and R-MOPS with PELT algorithm under $\alpha = 0.05$; (b) Autocorrelation of log-returns.

2005 was oil's tipping point.

References

- Baranowski, R., Chen, Y., and Fryzlewicz, P. (2019), "Narrowest-over-threshold detection of multiple change points and change-point-like features," *Journal of the Royal Statistical Society: Series B (Statistical Methodology)*, 81, 649{672.
- Barber, R. F., Candes, E. J., and Samworth, R. J. (2020), "Robust inference with knockoffs," *The Annals of Statistics*, 48, 1409{1431.
- Braun, J. V., Braun, R. K., and Müller, H. G. (2000), "Multiple changepoint fitting via quasilielihood, with application to DNA sequence segmentation," *Biometrika*, 87, 301{314.
- Fryzlewicz, P. (2020), "Detecting possibly frequent change-points: Wild Binary Segmentation 2 and steepest-drop model selection," *Journal of the Korean Statistical Society*, 1{44.
- Hao, N., Niu, Y. S., and Zhang, H. (2013), "Multiple change-point detection via a screening and ranking algorithm," *Statistica Sinica*, 23, 1553{1572.
- Murray, J. and King, D. (2012), "Oil's tipping point has passed," *Nature*, 481, 433{435.
- Petrov, V. (2002), "On probabilities of moderate deviations," *Journal of Mathematical Sciences*, 109, 2189{2191.
- Zou, C., Wang, G., and Li, R. (2020), "Consistent selection of the number of change-points via sample-splitting," *The Annals of Statistics*, 48, 413{439.